· Article · Advances in Polar Science
doi: 10.3724/SP.J.1085.2012.00087 June 2012 Vol. 23 No. 2: 87-94

Multiple processes affecting surface seawater N_2O saturation anomalies in tropical oceans and Prydz Bay, Antarctica

CHEN Liqi[1,2*], ZHAN Liyang[1,2], XU Suqing[1,2], ZHANG Jiexia[1,2], ZHANG Yuanhui[1,2] & XU Guojie[1,2]

[1] Key Laboratory of Global Change and Marine-Atmospheric Chemistry, State Oceanic Administration (SOA), Xiamen 361005, China;
[2] Third Institute of Oceanography, SOA, Xiamen 361005, China

Received 14 March 2012; accepted 5 April 2012

Abstract We analyzed the N_2O content of surface seawater sampled from Prydz Bay, Antarctica, on a cruise track between 30°S and 30°N during the twenty-second Chinese National Antarctic Research Expedition during austral summer, 2006. The surface water showed an average pN_2O value of 311.9±7.6 nL·L^{-1} (14.1±0.4 nmol·L^{-1}), which was slightly undersaturated. The air-sea N_2O flux in the region was -0.3±0.8 μmol·m^{-2}·d^{-1}; however, N_2O in the surface water was oversaturated in most stations along the cruise track. Saturation anomalies were greater than 10%, with a maximum of 54.7% being observed at the Equator, followed by 31% at 10°N in the Sulu Sea. The air-sea fluxes at these locations were 12.4 and 4 μmol·m^{-2}·d^{-1}, respectively. Overall, the results indicated that surface water in Prydz Bay was near equilibrium with atmospheric N_2O, and that ocean waters in lower latitudes acted as a N_2O source. Physical processes such as stratification, ice-melt water dilution, and solar radiation dominate the factors leading to N_2O saturation of surface water of Prydz Bay, while biological production and upwelling are primarily responsible for the N_2O oversaturation of surface water observed in subtropical and tropical regions along the cruise track.

Keywords **dissolved N_2O, saturation anomalies, tropic, subtropic, Prydz Bay**

Citation: Chen L Q, Zhan L Y, Xu S Q, et al. Multiple processes affecting surface seawater N_2O saturation anomalies in tropical oceans and Prydz Bay, Antarctica. Adv Polar Sci, 2012, 23: 87-94, doi:10.3724/SP.J.1085.2012.00087

0 Introduction

The atmospheric concentration and budget of N_2O is receiving increasing attention due to its effects on ozone depletion[1] and because it is a strong greenhouse effect with a molecule-for-molecule radiative forcing efficiency about 200—300 times greater than that of CO_2. The atmospheric N_2O mixing ratio has increased from a pre-industrial level of about 270±1 nL·L^{-1} to the current value of around 318—319 nL·L^{-1}[2] and continues to increase at about 0.25% per year[3]. The sharply increasing atmospheric N_2O mixing ratio in the past century may be in response to various anthropogenic activities, which contribute about 4.5±0.6 Tg·N·a^{-1} (Tg=10^{12}g, this unit means 10^{12}g per year). However, natural N_2O emissions still account for two thirds of the total emissions worldwide. For example, emissions from the ocean account for about 4 Tg·N·a^{-1} of N_2O[4]. These data indicate that oceanic N_2O exchange contributes significant amounts of N_2O to the atmospheric reservoir and acts as a net source for atmospheric N_2O.

Since the first study of N_2O by Craig and Gordon[5], considerable research has been conducted to investigate N_2O in the Pacific[6-13], Atlantic[14-18], Indian[19-27] and Southern Oceans[28-29]. Specifically, the studies that have been conducted to date were designed to better understand the possible mechanisms of N_2O production and factors that influence the distributions of N_2O in the ocean[12,30-31]. Isotopic techniques used to investigate the N_2O production

* Corresponding author (email: Lqchen@soa.gov.cn)

mechanism have shown that nitrification could be a dominant mechanism in N_2O production in open oceans[32-33]. However, other studies have suggested that denitrification could also be an important process in N_2O production[34]. More recently, the improvement of isotopic analytical techniques has enabled measurement of isotopomers, which could be used as evidence of the existence of nitrifier denitrification. Using this method, Charpentier et al.[35] suggested that nitrifier denitrification could be an important N_2O production pathway, even in oligotrophic and well-oxygenated waters.

Model studies contribute to our understanding of the distributions of N_2O. Nevison et al.[4] reported a N_2O flux of 1.2—6.8 $Tg{\cdot}N{\cdot}a^{-1}$ with an average of about 4 $Tg{\cdot}N{\cdot}a^{-1}$ from the world ocean, which agrees with the results of Suntharalingam and Sarmiento (3.85 $Tg{\cdot}N{\cdot}a^{-1}$)[36]. Taken together, these findings suggest that the ocean between 40°—60°S is a significant N_2O source, accounting for about one third of the global oceanic N_2O. Nevertheless, Nevison et al.[37] suggested that her previous work conducted in 1995 may overestimate the source strength of this area. This deviation might be due to a lack of data pertaining to the area. Clearly, further studies are necessary to better predict the N_2O air-sea flux and its variability throughout the world ocean.

Here, we present data obtained from Prydz Bay, Antarctica and along the cruise track between Fremantle, Australia and Shanghai, China during the twenty-second Chinese National Antarctic Research Expedition (22nd CHINARE) from January 15 to 25, and March 13 to 24, 2006. We also examine the differences in the distributions of surface water N_2O concentrations, saturation anomalies, and air-sea fluxes of different regions on the cruise based on these data.

1 Method

1.1 Study areas and methods

The sampling regions were located in Prydz Bay and on the cruise track between Fremantle and Shanghai (Figure 1a, 1b). The cruise track was divided into the following regions: West Coast of Australia (Stations 1–4), North Australian Basin (Stations 5–8), Lombok Strait (Stations 9–10), Makassar Strait (Stations 11–12), Celebes Sea (Stations 13–14), Sulu Sea (Stations 15–16), South China Sea (Stations 17–18), East China Sea (Stations 19–20).

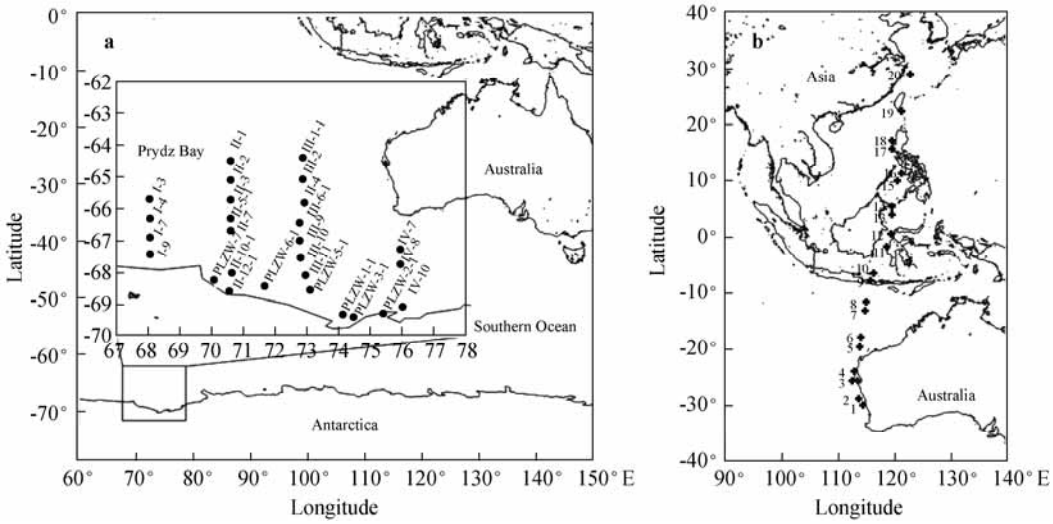

Figure 1 Location of study site and stations. **a**, Stations located in Prydz Bay. **b**, Stations located on the cruise track between Fremantle and Shanghai.

Seawater from a depth of about 6 m was continuously pumped. Triplicate water samples were collected and then treated and analyzed in the laboratory as described by Zhan and Chen[29].

1.2 Calculation and data processing

According to IPCC 2007 AR4, the mixing ratio of the N_2O atmospheric boundary layer is 318.5 $nL{\cdot}L^{-1}$[38]. N_2O Concentrations in the sea water were derived from the methods described by Weiss and Price[39]. Air-sea fluxes were calculated from equation (1):

$$F=k_w(C_a-C_w) \quad (1)$$

where, F is the flux ($\mu mol{\cdot}m^{-2}{\cdot}d^{-1}$), the seawater N_2O equilibrated concentration C_a is calculated from the boundary layer N_2O mixing ratio, and C_w is the observed *in situ* N_2O concentration in surface water. Additionally, the transfer velocity k_w was determined from the following equation (2):

$$k_w = k_{CO_2}(Sc_{N_2O}/Sc_{CO_2})^n \quad (2)$$

where, k_{CO_2} and Sc were calculated according to Liss and

Merlivat[40] and Wanninkhof[41], respectively.

1.3 Other data

SST (surface seawater temperature) and SSS (surface seawater salinity) data with intervals within 1/4° of the study areas were selected from data available at http://www.nodc.noaa.gov/OC5/SELECT/woaselect/woaselect.html, and interpolated to obtain the SST and SSS data for all stations on the cruise tracks. The surface water salinity and temperature in Prydz Bay were obtained from the Mark III CTD cast's measurement. The atmospheric pressure along the cruise tracks was measured every 10 min using the MILOS 500 meteorological monitoring system (Vaisala® Helsinki, Finland).

2 Results and discussion

According to Weiss and Price[39], the solubility of N_2O in surface seawater is strongly correlated with SST. However, deviation from equilibrium was observed in Prydz Bay and along the cruise track. The distribution patterns of N_2O in Prydz Bay and along the cruise track plotted against SST are shown in Figures 2 and 3. The *in situ* concentrations do not appear to be in equilibrium, which indicates that the distribution of N_2O may be influenced by other factors in addition to SST. To investigate these effects, we defined the saturation anomaly (SA) as equation (3):

$$SA=(C_s/C_e-1)\times 100=(S-1)\times 100 \quad (3)$$

where, the equilibrium concentration C_e (nmol·L^{-1}) is derived according to Weiss and Price[39], the proportion between C_s and C_e is the saturation of N_2O (S) in surface seawater, and the difference between this proportion and 1 (100%) is the SA. A value of 0 indicates that N_2O in the atmosphere and surface water is in equilibrium, while positive or negative values indicate that N_2O is oversaturated or undersaturated, respectively, in the surface water relative to the atmosphere.

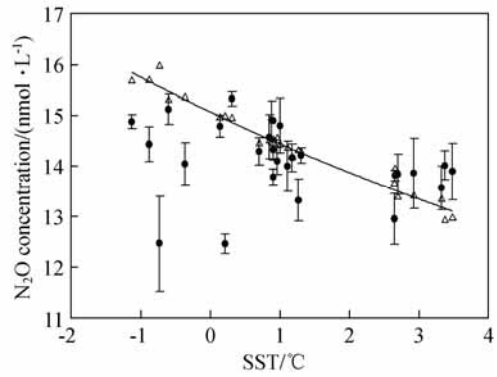

Figure 2 N_2O concentration (solid circles) in surface water vs. SST. An exponential function was fitted to the equilibrium concentrations (open triangles) for both Prydz Bay and the cruise track.

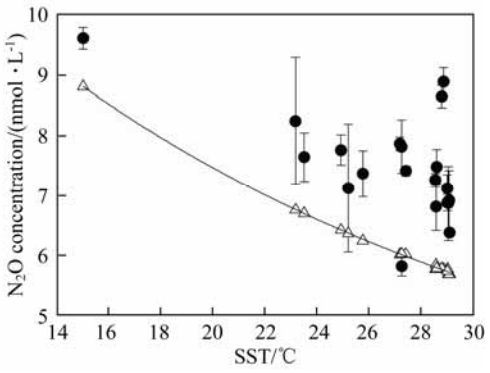

Figure 3 N_2O concentration (solid circles) in surface water vs. SST. An exponential function was fitted to equilibrium concentrations (open triangles) along the cruise track.

2.1 Pattern of dissolved N_2O in Prydz Bay and its air-sea fluxes

As shown in Figure 3, about two thirds of the measurements taken at stations in Prydz Bay showed an N_2O concentration lower than the equilibrium value, which suggests that the surface water of Prydz Bay is undersaturated with N_2O. Two areas with minimum values were found near 72°E and 74.5°E, where the N_2O concentration was about 12.5 nmol·L^{-1}. This concentration agrees well with data obtained from the Bellingshausen Sea[28] and McMurdo Sound[42]. N_2O production in the euphotic layer is inhibited by sunlight[43]; therefore, surface N_2O can only come from air-sea and surface-subsurface exchange. Phytoplankton blooming and subsequent remineralization in summer[44] probably enhance subsurface N_2O production in Prydz Bay. However, exchange between surface and subsurface waters is hampered in the bay by strong stratification during summer[44-45]; accordingly, N_2O can only be exchanged by eddy diffusion between these fractions during this period. It must also be assumed that subsurface biological processes contribute only a negligible amount of N_2O to surface water. Furthermore, the SST and SSS in Prydz Bay varied from -1.13℃—3.48℃ and 29.8—34.6, respectively (Figure 4a, 4b), which will have a significant impact on N_2O saturation. Zhan et al.[29] suggested that undersaturation may result from melting ice, and a similar phenomenon has been reported by Hamme and Emerson for inert gases[46]. However, as shown in Figure 5, no obvious relationship was observed between N_2O and SSS in Prydz Bay.

Dilution of surface water by sea-ice melt water may not be the only process that controls the surface water N_2O distribution pattern. To understand the processes controlling the distribution pattern, surface water was divided into three types of water masses in terms of SSS and SST, for which 34℃ and 0℃ were selected as the critical values, respectively. The three water masses were denoted type A (SSS≤34, SST≤0℃), type B (SSS≤34, SST>0℃), and type C (SSS>34, SST>0℃). As shown in Figure 5, N_2O saturation of water mass type A was well correlated with SSS (saturation is used instead of SA because SA could be

negative, which cannot be further fitted against SSS using an exponential growth equation). Below a certain temperature, saturation of dissolved N_2O should grow exponentially with increasing salinity. Since the temperature range of type A is within 1℃, we assumed that the effect of temperature on N_2O in water mass type A is negligible. An exponential curve was fitted to the saturation and salinity of type A water (R^2=0.985 4), suggesting that the N_2O saturation in this water type was dominated by ice-melt water.

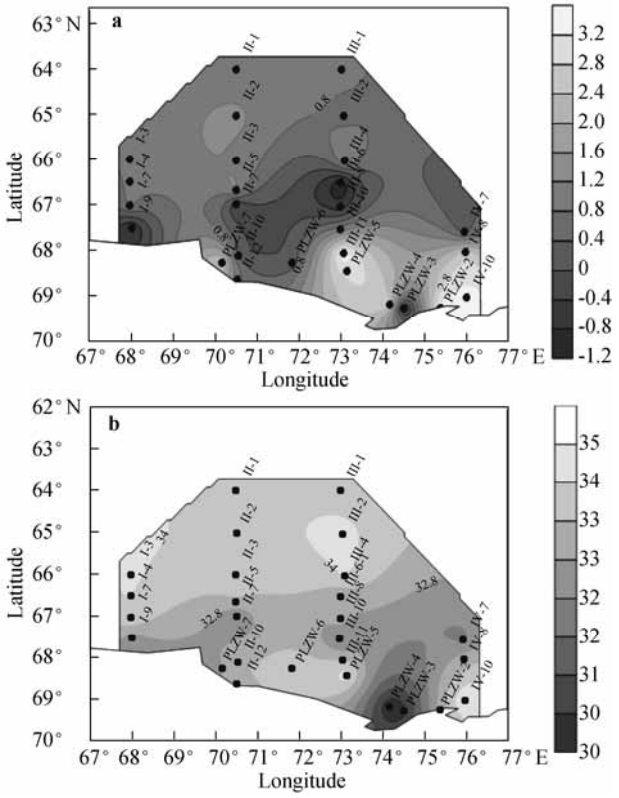

Figure 4 SST (**a**) and SSS (**b**) of Prydz Bay surface seawater during the expedition. The low salinity of Prydz Bay suggests that sea-ice melt water dilutes the surface water of Prydz Bay, especially around 74°E.

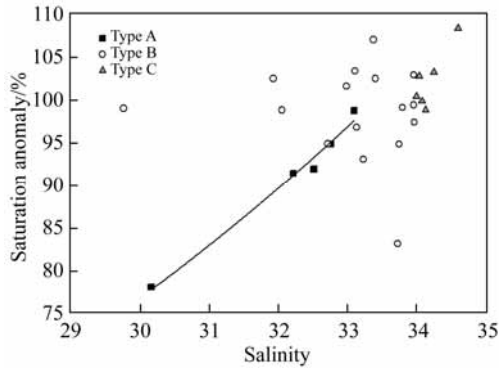

Figure 5 Saturation vs. salinity in Prydz Bay surface water. Three groups of water mass are divided and denoted as type A (SSS≤34, SST≤0℃), type B (SSS≤34, SST>0℃), and type C (SSS>34, SST>0℃). Type A was best fitted with an exponential growth equation $f(x)= \exp[a(x-x_0)]$ (R^2 = 0.985 4).

To quantify the impact of ice melting on the saturation anomaly, the following mass balance equations were set:

$$f_1S_1+f_2S_2=S_{\mathrm{mix}} \tag{4}$$

$$f_1C_1+f_2C_2=C_{\mathrm{mix}} \tag{5}$$

$$f_1T_1+f_2T_2=T_{\mathrm{mix}} \tag{6}$$

$$f_1+f_2=1 \tag{7}$$

where, f_1 and f_2 are fractions of two end members: Sea-ice meltwater and seawater. One end member consisted of the salinity S_1 and temperature T_1 of ice-melt water, which are 4 and -1.9℃, respectively. The other end member consisted of S_2 and T_2, which are the SSS and SST of end member water from various stations. Because variations in salinity only introduce marginal error to calculation of the N_2O concentration in seawater end members, salinity S_2 is taken as 34, which is typical of surface water south of the Polar Front, which is unaffected by sea-ice melt water. Temperature T_2 can be calculated from equation (6), C_1 is the concentration of N_2O in sea-ice melt water, which is assumed to be zero because the formation is a degassing process, and C_2 is the equilibrium concentration of the other end member before it mixes with ice-melt water.

T_{mix} and S_{mix} are the SST and SSS after mixing of the two end members, or the *in situ* SST and SSS. Saturation anomalies of different stations of type A can be calculated using the following equation:

$$\mathrm{SA}=C_{\mathrm{mix}}/C\ (T_{\mathrm{mix}},\ S_{\mathrm{mix}})-1 \tag{8}$$

where, C_{mix} is calculated from equation (5), and C (T_{mix}, S_{mix}) is the equilibrium concentration of the two-end-member mixture, which is derived from *in situ* temperature T_{mix} and salinity S_{mix}. All of the calculated saturation anomalies listed in Table 1 are within 5% of their observed counterparts. The calculated and observed values are correlated with each other and have R^2 values as high as 0.991 9 (Figure 6). These results also suggest that N_2O in water mass type A is dominated by sea-ice dilution.

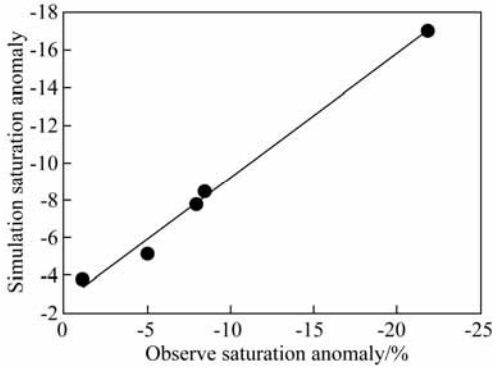

Figure 6 Correlation between simulation saturation anomalies and observed saturation anomalies in Prydz Bay (R^2 = 0.991 9).

The distribution of N_2O in water mass type B shows a

different pattern. Specifically, no relationship was observed between N_2O and salinity (Figure 5), and the saturation value was around 100%, suggesting that this type of water is near saturation. Additionally, this water mass has lower salinity, which suggests that it underwent ice-melt water dilution, was then heated by solar radiation, and finally re-equilibrated with atmospheric N_2O.

Table 1 Observed saturation and simulated saturation anomalies

Stations	Observed saturation anomaly/%	Simulated saturation anomaly/%	Absolute deviation /%
PLZW-3-1-a	-21.9	-17.1	4.8
II-7-a	-8.5	-8.5	0.0
I-9-a	-8.0	-7.8	0.2
III-6-1-a	-5.1	-5.2	0.1
III-9-a	-1.2	-3.8	2.6

The SSS of water mass type C is greater than 34. This water mass may be unaffected or only mildly affected by ice-melt seawater. The increasing SST and SSS in type C water and their positive correlation suggest that this water mass may have been warmed by solar radiation, resulting in some evaporation. Salinity only changed within a range of 0.6, suggesting a negligible contribution to N_2O saturation anomalies; therefore, the anomaly would primarily be affected by SST. The SST of type C water ranges within 2.7℃ (0.7℃—3.4℃), which corresponds to a difference of 9.7% between saturation anomalies. These findings agree well with the *in situ* difference of 10% observed between the highest and lowest SA in water mass type C and suggest that N_2O in water mass type C is primarily controlled by solar radiation.

Based on equations (1) and (2), the calculated average flux of N_2O in Prydz Bay was -0.3±0.8 $\mu mol \cdot m^{-2} \cdot d^{-1}$ during the survey period. These results indicate that the N_2O in the surface seawater of Prydz Bay is nearly in equilibrium with the atmospheric mixing ratio during summer, while there is nearly no sea to air input of N_2O in this area.

2.2 Pattern of dissolved N_2O and its air-sea fluxes

The N_2O saturation anomalies of surface seawater measured at most stations along the cruise track were greater than 10%, with the exception of a value of -3.5% recorded at 16.72°N. Maximum values greater than 50% and 30% were found at the equator and around 10°N, respectively (Figure 7). Variations in the saturation of N_2O in the surface water measured along the cruise track could have many origins, such as differences in hydrographical or biogeochemical properties at different latitudes.

2.2.1 North Australia Basin

Data pertaining to the south end of the cruise track near the coast of Western Australia (Figure 8) suggest that the saturation anomaly could be explained by seasonal thermal deviation of surface seawater[29]. Variations in the temperature of coastal surface water at around 30°S can be as high as 7℃. Such variations would result in a saturation anomaly of approximately 21%, which is consistent with the observations of the present study.

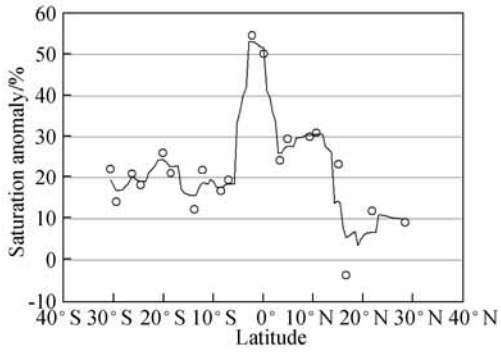

Figure 7 Saturation anomaly measured along the cruise track between Fremantle and Shanghai. Maximum values were observed between the equator and 10°N.

Fieux et al.[47] revealed that a sharp front existed during both summer and winter at around 13°S to 14°S, which is also demonstrated by the SSS turning point at approximately the same latitude (Figure 8). South of this front are high salinity subtropical waters produced by higher evaporation rates, while low salinity water from Indonesia flows to the north. However, the measured saturation anomaly does not appear to be different from that other stations in the North Australia Basin.

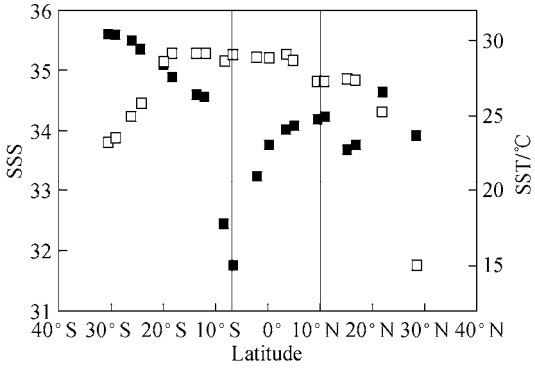

Figure 8 SST (open squares) and SSS (solid squares) measured along the cruise track. Three obvious hydrographic regimes are marked from left to right with straight lines.

2.2.2 Makassar Strait

The highest N_2O saturation anomaly was observed in the Makassar Strait, around the Equator. Since seasonal thermal effects could only account for 6% of the saturation anomaly in equatorial regions, the remaining 44% of the anomaly must be explained by other oceanic processes such as variations in SST, SSS, ocean currents, and possible biological activity.

The hydrographic characteristics of the Makassar Strait could influence the saturation anomaly. The Makassar Strait is a westerly path for the Indonesia Through Flow (ITF). The vertical profile of the Makassar Strait reflects characteristics of different origins. The surface water is freshened by Mahakam River runoff during the Northwest Monsoon (NWM), when samples of this region were collected. This could explain why the lowest salinity was observed between 30°S and 30°N (Figure 8)[48]. The highest N_2O saturation anomaly found on the salinity front along the cruise track suggests a possible strong biological N_2O contribution during mixing processes.

2.2.3 Sulu Sea

Another N_2O saturation anomaly maximum was observed in the north Sulu Sea around 10°N. The saturation anomaly value was as high as 31%, which was the largest value measured during cruise. This anomaly may have resulted from upwellings in this region, as indicated by SST and SSS data along the cruise track (Figure 8). The SST and SSS curves show a trough and a crest, respectively, at around 10°N. Additionally, this region had lower temperature and higher salinity, suggesting that upwelling was occurring. These findings are consistent with those of Wang et al.[49], who found that during austral winter (November to April), strong northeast winds drive the upwelling of cold and nutrient rich water from lower depths to the upper layer in the north Sulu Sea. N_2O could also be brought to the surface during this process.

2.2.4 South China Sea and East China Sea

The lowest saturation anomaly of -3.5% was observed at 16.7°N, at the eastern boundary of the South China Sea, indicating that the surface water N_2O was nearly in equilibrium with the atmosphere. Relatively low salinity values were also found at this latitude (Figure 8) corresponding to river runoff. However, no obvious increase in the saturation anomaly related to runoff or other biological or physical processes was observed in this region.

The saturation anomaly values measured at stations located in the east of Taiwan and in the East China Sea were both around 10%. The SST east of Taiwan showed no significant changes between March and December, suggesting that there is a source at this latitude during early spring.

2.3 Air-sea fluxes along the cruise track

The air-sea fluxes measured between Fremantle and Shanghai fluctuated along the cruise track (Figure 9), with the highest value of 12.4 $\mu mol \cdot m^{-2} \cdot d^{-1}$ being observed at around 10°N, possibly reflecting the combined effects of upwelling in the north Sulu Sea and high wind speed. The second highest value was observed at around 30°N, which likely resulted from the high wind speed at this latitude. No significant air-sea N_2O flux was observed between 0°—10°S, although the highest saturation anomaly of the entire cruise track was observed at the Equator. Another low value was observed at 16.7°N, resulting from both low saturation anomaly and low wind speed at this latitude.

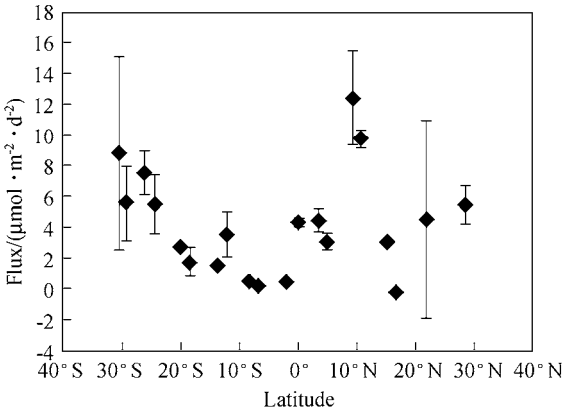

Figure 9 Air-sea fluxes of N_2O between Fremantle and Shanghai.

3 Conclusions

Analyses of surface seawater samples collected in Prydz Bay during the 22nd CHINARE cruise between January and March 2006 indicated that the seawater was nearly in equilibrium with the atmospheric N_2O mixing ratio, with an average concentration of 14.1±0.4 $nmol \cdot L^{-1}$, or 311.9± 7.6 $nL \cdot L^{-1}$ after conversion to partial pressure under in-situ conditions. When compared with the atmospheric mixing ratio of 318.5 $nL \cdot L^{-1}$, the surface seawater is slightly undersaturated, with an average air-sea N_2O flux of -0.3± 0.8 $\mu mol \cdot m^{-2} \cdot d^{-1}$ during the period. The complicated distribution pattern of N_2O saturation anomalies in the seawater may have resulted from a combination of physical processes. The dilution of surface water by sea ice meltwater with a lower N_2O would result in N_2O undersaturaton. The mixture of sea ice meltwater and surface seawater in open water was further warmed by solar radiation, which enabled re-equilibration with the atmosphere. Some surveyed regions with an SST of greater than 3℃ SST showed no significant impact from sea ice meltwater and resulted in N_2O oversaturation in this region.

In contrast to Prydz Bay, surface seawater samples collected between Fremantle and Shanghai were supersaturated with N_2O, indicating that this area behaved as a source for atmospheric N_2O. Saturation anomalies in most of the surface water samples were greater than 10%, with the highest value of 54.7% being observed at the Equator, and the second highest value of 31% occurring at about 10°N in the Sulu Sea. No significant sources of N_2O were observed in the North Australia Basin or East China Sea. The highest values may have primarily resulted from subsurface production, upwelling or both of these factors; however, the air-sea fluxes of these two locations were reversed relative to their saturation anomalies, with values of 12.4 $\mu mol \cdot m^{-2} \cdot d^{-1}$ and less than 4 $\mu mol \cdot m^{-2} \cdot d^{-1}$, respectively. This difference may be attributed to wind speed.

Acknowledgements Data issued by the Data-sharing Platform of Polar Science (http://www.chinare.org.cn) maintained by Polar Research Institute of China (PRIC) and Chinese National Arctic & Antarctic Data Center (CN-NADC). This research was jointly sponsored by the National Natural Science Foundation of China (Grant nos. 40671062, 41106168), the National High Technique Research & Development Program of China (Grant no. 2008AA121703), the Ministry of Science and Technology of China (Grant nos. 2004DIB5J178, 2009DFA22920) and the Chinese Arctic and Antarctic Administration (CAA) Cooperation Program (Grant nos. IC2010013, IC2011114, IC201201).

References

1 Crutzen P J. The influence of nitrogen oxides on the atmospheric ozone content. Quarterly Journal of the Royal Meteorological Society, 1970, 96: 320-325.
2 Forster P, Ramaswamy V, Artaxo P, et al. Climate Change 2007: the physical science basis//Solomon S, Qin D, Manning M, et al. Contribution of working Group I to the Fourth Assessment Report of the Intergovernmental Panel on Climate Change. Cambridge: Cambridge University Press, 2007: 129-234.
3 Khalil M A K, Rasmussen R A. The global sources of nitrous oxide. Journal of Geophysical Research, 1992, 97: 14651-14660.
4 Nevison C D, Weiss R F, Erickson III D J, et al. Global oceanic emissions of nitrous oxide. Journal of Geophysical Research, 1995, 100: 15809-15820.
5 Craig H, Gordon L I. Nitrous oxide in the ocean and the marine atmosphere. Geochimica et Cosmochimica Acta, 1963, 22: 949-955.
6 Cohen Y. Consumption of dissolved nitrous oxide in an anoxic basin, Saanich Inlet, British Columbia. Nature, 1978, 272: 235-237.
7 Cohen Y, Gordon L I. Nitrous oxide production in the ocean. Journal of Geophysical Research, 1979, 84: 347-353.
8 Cohen Y, Gordon L I. Nitrous oxide in the oxygen minimum of the eastern tropical North Pacific: Evidence for its consumption during denitrification and possible mechanisms for its production. Deep-Sea Research, 1978, 25: 509–524.
9 Singh H B, Salas L J, Shigeishi H. The distribution of nitrous oxide/N_2O/ in the global atmosphere and the Pacific Ocean. Tellus, 1979, 31: 313-320.
10 Pierotti D, Rasmussen R A. Nitrous oxide measurements in the eastern tropical Pacific Ocean. Tellus, 1980, 32: 56-72.
11 Butler J, Elkins J W, Thompson T M, et al. Tropospheric and dissolved N_2O of the West Pacific and East Indian Oceans during the El Nino southern oscillation event of 1987. Journal of Geophysical Research, 1989, 94: 14865-14877.
12 Codispoti L A, Christensen J P. Nitrification, denitrification and nitrous oxide cycling in the eastern tropical South Pacific Ocean. Marine Chemistry. 1985, 16: 277-300.
13 Dore J E, Popp N, Karl D M, et al. A large source of atmospheric nitrous oxide from subtropical North Pacific surface waters. Nature, 1998, 396: 63-66.
14 Hahn J. The North Atlantic Ocean as a source of atmospheric N_2O. Tellus, 1974, 26:160-168.
15 Oudot C, Anderie C, Montel Y, et al. Nitrous oxide production in the tropical Atlantic Ocean. Deep-Sea Research, 1990, 37: 183-202.
16 Oudot C, Jean-Baptiste P, Fourré E C, et al. Transatlantic equatorial distribution of nitrous oxide and methane. Deep-Sea Research Part I, 2002, 49: 1175-1193.
17 Morell J M, Capella J, Mercado A, et al. Nitrous oxide fluxes in Caribbean and tropical Atlantic waters: evidence for near surface production. Marine Chemistry, 2001, 74: 131-143.
18 Walter S, Bange H W, Reitenbach U B, et al. Nitrous oxide in the North Atlantic Ocean. Biogeosciences, 2006, 3: 607-619.
19 Law C S, Owens N J P. Significant flux of atmospheric nitrous oxide from the northwest Indian Ocean. Nature, 1990, 346: 826-828.
20 Wilde H P J, Helder W. Nitrous oxide in the Somali Basin: the role of upwelling. Deep-Sea Research Part II, 1997, 44: 1319-1340.
21 Bange H W, Rapsomanikis S, Andreae M. Nitrous oxide emissions from the Arabian Sea. Geophysical Research Letters, 1996, 23: 3175-3178.
22 Lal S, Patra P K. Variabilities in the fluxes and annual emissions of nitrous oxide from the Arabian Sea. Global Biogeochemical Cycles, 1998, 12: 321-327.
23 Bange H W, Rapsomanikis S, Andreae M. Nitrous oxide emissions from the Arabian Sea: A synthesis. Atmospheric Chemistry and Physics, 2001, 1: 61-71.
24 Patra P K, Lal S. Seasonal and spatial variability in N_2O distribution in the Arabian Sea. Deep-Sea Research Part I, 1999, 46: 529-543.
25 Naqvi S W A, Noronha R J. Nitrous oxide in the Arabian Sea. Deep-Sea Research Part A: Oceanographic Research Papers, 1991, 38: 871-890.
26 Naqvi S W A, Jayakumar D A, Narvekar P V, et al. Increased marine production of N_2O due to intensifying anoxia on the Indian continental shelf. Nature, 2000, 408: 346-349.
27 Naqvi S W A, Bange H W, Gibb S W, et al. Biogeochemical ocean-atmosphere transfers in the Arabian Sea. Progress in Oceanography, 2005, 65: 116-144.
28 Rees A P, Owens N J P. Nitrous oxide in the Bellingshausen Sea and Drake Passage. Journal of Geophysical Research, 1997, 102: 3383-3392.
29 Zhan L, Chen L. Distributions of N_2O and its air-sea fluxes in seawater along cruise tracks between 30°S—67°S and in Prydz Bay, Antarctica. Journal of Geophysical Research, 2009, 114, C03019.
30 Yoshinari T. Nitrous oxide in the sea. Marine Chemistry, 1976, 4: 189-202.
31 Elkins J W, Wofsy S C, McElroy M B, et al. Aquatic sources and sinks for nitrous oxide. Nature, 1978, 275: 602-606.
32 Yoshida N, Hattori A, Toshiro S, et al. $^{15}N/^{14}N$ ratio of dissolved N_2O in the eastern tropical Pacific Ocean. Nature, 1984, 307: 442-444.
33 Yoshida N, Hattori A, Saino T, et al. ^{15}N-depleted N_2O as a product of nitrification. Nature, 1988, 335: 528-529.
34 Yoshida N, Morimoto H, Hirano M, et al. Nitrification rates and ^{15}N abundances of N_2O and NO_3^- in the western North Pacific. Nature, 1989, 342: 895-897.
35 Charpentier J, Farias L, Yoshida N, et al. Nitrous oxide distribution and its origin in the central and eastern South Pacific Subtropical Gyre. Biogeosciences, 2007, 4: 729-741.
36 Suntharalingam P, Sarmiento J L. Factors governing the oceanic nitrous oxide distribution: Simulations with an ocean general circulation model. Global Biogeochemical Cycles, 2000, 14: 429–454.
37 Nevison C D, Keeling R F, Weiss R F, et al. Southern Ocean ventilation inferred from seasonal cycles of atmospheric N_2O and O_2/N_2 at Cape Grim, Tasmania. Tellus B, 2005, 57: 218-229.
38 IPCC. Climate Change 2007: The Scientific Basis. Contribution of Working Group I to the Fouth Assessment Report of the Intergovernmental Panel on Climate Change//Houghton J T, et al. Cambridge: Cambridge University Press, 2007.
39 Weiss R F, Price B A. Nitrous oxide solubility in water and seawater. Marine Chemistry, 1980, 8: 347-359.
40 Liss P S, Merlivat L. The role of air-sea exchange in geochemical cycling//Buat-Menard P, Reiel D, Dordrechl. Holland, 1986: 113-127.
41 Wanninkhof R. Relationship between wind speed and gas exchange. Journal of Geophysical Research, 1992, 97: 7373-7382.
42 Priscu J C, Downes M T, McKay C P. Extreme supersaturation of nitrous oxide in a poorly ventilated Antarctic lake. Limnology and Oceanography, 1996, 41: 1544-1551.

43 Olson R J. Differential photoinhibition of marine nitrifying bacteria: a possible mechanism for the formation of the primary nitrite maximum. Journal of Marine Research, 1981, 39: 227-238.

44 Gibson J A E, Trull T W. Annual cycle of fCO_2 under sea-ice and in open water in Prydz Bay, East Antarctica. Marine Chemistry, 1999, 66: 187-200.

45 Smith N R, Dong Z Q. Water masses and circulation in the region of Prydz Bay, Antarctica. Deep-Sea Research Part A. Oceanographic Research Papers, 1984, 31: 1121-1147.

46 Hamme R C, Emerson S R. Mechanisms controlling the global oceanic distribution of the inert gases argon, nitrogen and neon. Geophysical Research Letters, 2002, 29: 2120.

47 Fieux M, Andrié C, Charriaud E. Hydrological and chlorofluoromethanes measurements at the entrance of the throughflow into the Indian Ocean. Journal of Geophysical Research, 1995, 101(C5): 12433-12454.

48 Kinkade C, Marra J, Langdon C, et al. Monsoonal differences in phytoplankton biomass and production in the Indonesian Seas: tracing vertical mixing using temperature. Deep-Sea Research, 1997, 44: 581-592.

49 Wang J, Qi Y Q, Jones S F. An analysis of the characteristics of chlorophyll in the Sulu Sea. Journal of Marine Systems, 2006, 59: 111-119.